# Nonlinear interlayer tunneling in a double-electron-layer structure

S. K. Lyo

*Sandia National Laboratories, Albuquerque, New Mexico 87185*

(Received 2 August 1999)

We present a theory for nonequilibrium two-dimensional to two-dimensional tunneling between two weakly tunnel-coupled electron layers when the chemical potentials of the two electron gases are arbitrarily biased. We first present an intuitive but rigorous second-order perturbation theory based on a transition-rate approach. Contributions from electron-impurity, interface-roughness, electron-electron, and electron-phonon interactions are considered. The validity of this result is established using a more general field-theoretic formalism by expressing the tunneling current as a current-current correlation function which can be evaluated employing a standard temperature-ordered Green's function technique and a Feynman-graph expansion. The formalism is exact to the second order in the tunneling integral and to all orders in the interactions and is useful for studying higher-order interaction effect. The relevance of the numerical results to recent experimental data from a GaAs/Al$_x$Ga$_{1-x}$As double-electron-layer tunneling transistor (DELTT) at 77 K are discussed. These data show a large peak-to-valley ratio of the $I$-$V$ curve. The room-temperature numerical results for the $I$-$V$ curve show a reasonably large peak-to-valley ratio indicating the feasibility of room-temperature DELTT's.

## I. INTRODUCTION

Currently, there has been an increasing interest in the tunneling phenomenon between two quasi-two-dimensional (2D) layers of electron gases separated by a wide barrier.[1–7] This phenomenon is not only interesting academically but also offers potentially valuable application to 2D-2D tunneling transistors which have sharp current-voltage characteristics owing to the restricted phase space available for tunneling compared to the conventional transistors based on 3D-2D tunneling.[8–10] This effect has recently been demonstrated by Simmons *et al.*[11] This paper presents a theory for tunneling for the double-quantum-well (DQW) 2D-2D tunneling structure pioneered by Eisenstein, Pfeiffer, and West.[3] In this structure, the two QW's have independent Ohmic contacts. When a bias potential $V$ is applied between the source and the drain contacts, the electrons drift into the top QW (QW1), tunnel through the wide center barrier into the bottom QW (QW2) and flow out of QW2. The two QW's are not in equilibrium, with the difference of their chemical potentials $\mu_1$ and $\mu_2$ given by $\mu_1 - \mu_2 = eV (\geq 0)$. In this paper, we obtain the tunneling current as a function of $eV$ assuming that the in-plane conductances of the QW's are vary large, causing a significant potential drop only over the barrier. The effect of in-plane resistance on the source-drain $I$-$V$ curve can be studied using the $I$-$V$ relationship obtained here and a differential transmission line model.[6]

The present model is very relevant to the GaAs/Al$_x$Ga$_{1-x}$As double-electron-layer tunneling transistor (DELTT) recently developed by Simmons *et al.*[11] This structure is very similar to that studied by Eisenstein *et al.*[4] but (1) with a much smaller gate size allowing only a small potential drop in the QW's, and (2) with a nonlinear source-drain bias $V$. The DELTT structure is free from space-charge effects[11] because the current exits the second (i.e., drain) QW immediately after tunneling through the barrier. On the other hand, space-charge effects change the $I$-$V$ characteristics in

3D-2D transistors, where charge can be accumulated in the QW.[12]

Of particular interest in this paper is the investigation of the maximum possible temperature-dependent peak-to-valley ratio in a given structure in the ideal intrinsic limit, namely, in the limit where the major effect from the static scattering centers are eliminated through modulation doping. This requires a careful microscopic treatment of the level damping arising from the intrinsic scattering mechanism such as electron-electron and electron-phonon interactions. Line-shape broadening due to extrinsic static scattering such as impurity or interface-roughness scattering is considered formally. The effect is sample dependent and will be treated phonomenologically to compare the theoretical results with data.

The present paper is structured as follows. We formulate the tunneling current in terms of an intuitive second-order transition-rate theory using a $T$-matrix approach in Sec. II. Contributions from electron-impurity (or-surface roughness), electron-electron, and electron-phonon interactions are considered. The validity of the results in Sec. II is examined in Sec. III, where we establish a formal theory of the nonequilibrium 2D-2D tunneling current in terms of the current-current correlation function. This is then evaluated employing a standard temperature-ordered Green's function technique and a graph expansion. The formalism is exact to the second order in the tunneling integral $J$ and to all orders in the interactions and is similar to the linear response theory. The formalism is valid in the limit where $J$ is small (i.e., $\ll$ damping $\Gamma$), namely, when the tunneling time is much longer than the scattering time. This limit corresponds to sequential tunneling in the double-barrier tunneling system. This condition is well satisfied in typical tunneling transistors, where the center barrier is wide allowing the charges in the two QW's to be controlled independently. Numerical results are given in Sec. IV and compared with recent experimental data from GaAs/Al$_x$Ga$_{1-x}$As DELTT available at 77 K. The $I$-$V$ curve is also evaluated at 300 K in order to

assess the feasibility of room-temperature DELTT. The paper is concluded in Sec. V with a brief discussion.

## II. TRANSITION-RATE FORMALISM

The Hamiltonian is given, in the absence of tunneling, by

$$H = \sum_{j=1,2} \sum_k \varepsilon_{jk} a_{jk}^\dagger a_{jk} + \sum_{sq} \hbar \omega_{sq}(b_{sq}^\dagger b_{sq} + 1/2) + H_{im}$$
$$+ H_{e\text{-ph}} + H_{e\text{-}e}, \tag{1}$$

where $\varepsilon_{jk}$ is the electron energy for the wave vector **k** in the $j$th QW, $a_{jk}^\dagger$ ($a_{jk}$) is the fermion creation (destruction) operator, $\hbar \omega_{sq}$ is the phonon energy of mode $s$ and wave vector **q**, and $b_{sq}^\dagger$ ($b_{sq}$) is the boson creation (destruction) operator. The rest of the terms in Eq. (1) denote electron interactions with the impurities, LO phonons, acoustic phonons, and other electrons. The expressions for these terms will be given later. The spin sum is suppressed. The total Hamiltonian is the sum of $H$ and the tunneling Hamiltonian $H_{tun}$:

$$H_{tun} = t + t^\dagger; t = J \sum_k a_{1k}^\dagger a_{2k}, \tag{2}$$

where $J$ is the tunneling integral. The operator $t(t^\dagger)$ transfers an electron from QW2 (QW1) to QW1 (QW2). While we concentrate on the ground sublevels of each QW, the result can be generalized to include tunneling between all the sublevels if the index $k$ includes the sublevel index implicitly. In this case, $J$ depends on the sublevel indices.

In general, tunneling cannot occur directly from an initial state $|1k\rangle$ in QW1 to a final state $|2k\rangle$ in QW2, because momentum and energy conservation cannot be satisfied simultaneously when the energy dispersions $\varepsilon_{1k}$ and $\varepsilon_{2k}$ are not aligned (i.e., $\varepsilon_{1k} \neq \varepsilon_{2k}$). Here $|jk\rangle$ is the noninteracting eigenstate of the first term of $H$. We therefore need to construct second-order perturbation processes through which momentum and energy can be dissipated. We use a second-order perturbation theory which treats the resonance in the intermediate energy denominators rigorously.[13] An alternate more general and formal diagrammatic approach useful for a systematic study of higher-order effects is presented in Sec. III.

### A. Tunneling through electron-impurity scattering

Figure 1 shows second-order perturbation processes which allow an electron to tunnel from an initial state $|1k\rangle$ to a final state $|2k'\rangle$. In Fig. 1(a), the electron is first scattered (indicated by the black dot) into an intermediate state $|1k'\rangle$ and then tunnels into $|2k'\rangle$. In Fig. 1(b), the electron first undergoes virtual tunneling into an intermediate state $|2k\rangle$ and then is scattered into the final state $|2k'\rangle$. In this elastic transition, momentum is dissipated through impurity collisions in QW1 [Fig. 1(a)] as well as in QW2 [Fig. 1(b)]. The $T$ matrix for these processes is given by[13]

$$T_{1k\to2k'}^{im} = \frac{J\langle 1k'|\tilde{H}_{im}|1k\rangle}{\varepsilon_{1\kappa} - \varepsilon_{1\kappa'} - i\Gamma_{1\kappa'}(\varepsilon_{1\kappa})} + \frac{\langle 2k'|\tilde{H}_{im}|2k\rangle J}{\varepsilon_{1\kappa} - \varepsilon_{2k} - i\Gamma_{2k}(\varepsilon_{1\kappa})}, \tag{3}$$
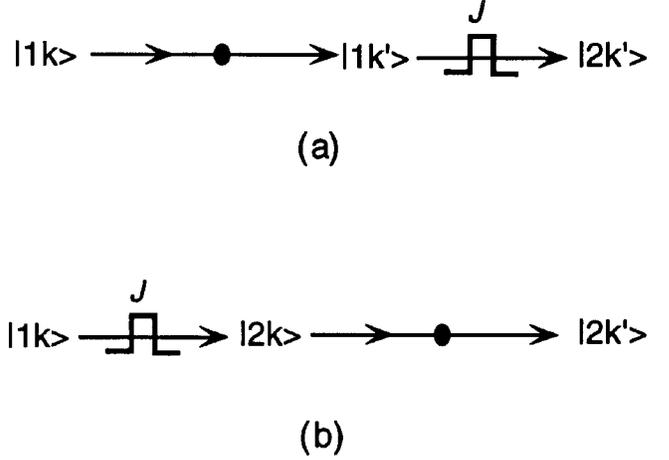


**(a)**



**(b)**

FIG. 1. Second-order two-step processes for tunneling through electron-impurity and electron-phonon interactions (black dots). Tunneling takes place (a) after and (b) before the interaction.

where $\tilde{H}_{im}$ is the sum of the screened impurity potentials and the interface-roughness potentials. In Eq. (3), intermediate-state damping $\Gamma_{jk}(z)$ is included for resonant transitions. The argument $z$ of the damping $\Gamma_{jq}(z)$ for the $T$ matrix in Eq. (3) as well as for the $T$ matrices for the electron-phonon and electron-electron processes to be introduced later is determined from the fact that the denominator in the first and second term of Eq. (3) is the denominator of the Green's function of the intermediate states $|jq\rangle = |1k'\rangle$ and $|jq\rangle = |2k\rangle$, respectively, namely $G_{jq}(z-i0) = [z - \varepsilon_{jq} - i\Gamma_{jq}(z)]^{-1}$, ignoring the energy shift. Hence, $z = \varepsilon_{1k}$ for both terms of Eq. (3). Note that, in the present nonequilibrium tunneling problem, the $z$ and $k$ dependences of $\Gamma_{jk}(z)$ are important and make the problem more complicated than in the linear response case where only the properties on the Fermi surface matter.

The transition rate from QW1 to QW2 is then given by

$$W_{1\to2}^{im} = \frac{4\pi}{\hbar} \sum_{kk'} f_{1k}(1-f_{2k'})\langle |T_{1k\to2k'}^{im}|^2\rangle_{im} \delta(\varepsilon_{1k} - \varepsilon_{2k'}). \tag{4}$$

Here, a factor of 2 is included for the spin degeneracy and $\langle \rangle_{im}$ denotes impurity averaging. The back-transition rate $W_{2\to1}^{im}$ can be found in a similar way. Subtracting the back-transition rate from Eq. (4), assuming an in-plane inversion symmetry (i.e., $\varepsilon_{j-k} = \varepsilon_{jk}$), and multiplying the rate by the electron charge $e$, we find the tunneling current

$$I^{im} = \frac{4\pi e J^2}{\hbar} F(V) \sum_{kk'} f_{1k}(1-f_{2k'}) \left\langle \left| \frac{\langle 1k'|\tilde{H}_{im}|1k\rangle}{\Delta - i\Gamma_{1k'}} \right. \right.$$
$$\left. \left. + \frac{\langle 2k'|\tilde{H}_{im}|2k\rangle}{-\Delta - i\Gamma_{2k}} \right|^2 \right\rangle_{im} \delta(\varepsilon_{1k} - \varepsilon_{2k'}), \tag{5}$$

where $F(V) = 1 - \exp(-\beta eV)$, $f_{jk}$ is the Fermi function $f_{jk} = \{\exp[\beta(\varepsilon_{jk} - \mu_j)]+1\}^{-1}$, $\beta = k_BT$, $T$ is the temperature, $\Delta = \varepsilon_{2k} - \varepsilon_{1k} = \Delta_0 - eV$ and $\Gamma_{jk} \equiv \Gamma_{jk}(\varepsilon_{j*k})$ with the understanding $1* \equiv 2$, and $2* \equiv 1$. $\Delta_0$ is the difference of the ground sublevels of the two QW's in the absence of the bias. For zero bias $V = 0$, we have $F(V) = 0$, yielding $I^{im} = 0$ due

to detailed balance. It turns out that the energy denominators for the intermediate states in Eq. (5) have the same expression for tunneling through electron-phonon interaction (EPI) and electron-electron interaction as will be shown later.

## B. Tunneling through electron-phonon scattering

Phonon-assisted tunneling is obtained from the same processes illustrated in Fig. 1 except that the black dots now indicate phonon absorption and emission. The initial state $|1k,n_{sq}\rangle$ consists of an electron in $|1k\rangle$ and phonons in $|n_{sq}\rangle$. The final state is $|2k',n_{sq}\pm1\rangle$ depending on whether a phonon is emitted $(+)$ or absorbed $(-)$. In Fig. 1(a), the electron is first scattered into an intermediate state $|1k',n_{sq}\pm1\rangle$ through virtual (or real) phonon emission or absorption and then tunnels into $|2k'\rangle$. In Fig. 1(b), the electron first undergoes virtual tunneling into an intermediate state $|2k\rangle$ and then is scattered into the final state $|2k',n_{sq}\pm1\rangle$ emitting or absorbing a phonon of mode $sq$. In this inelastic transition, energy and momentum are transferred to the phonon bath. The $T$ matrix equals

$$
T^{ph\pm}_{1k\to2k'}(sq)=\frac{J\langle1k',n_{sq}\pm1|\tilde{H}^{\pm}_{e\text{-}ph}|1k,n_{sq}\rangle}{\varepsilon_{1\kappa}-(\varepsilon_{1\kappa'}\pm\hbar\omega_{sq})-i\Gamma_{1k'}(\varepsilon_{1\kappa}\mp\hbar\omega_{sq})}
$$
$$
+\frac{\langle2k',n_{sq}\pm1|\tilde{H}^{\pm}_{e\text{-}ph}|2k,n_{sq}\rangle J}{\varepsilon_{1\kappa}-\varepsilon_{2k}-i\Gamma_{2k}(\varepsilon_{1\kappa})}, \quad (6)
$$

where $n_{sq}=[\exp(\beta\hbar\omega_{sq})-1]^{-1}$ is the boson function. The arguments of the damping in Eq. (6) are determined according to the method discussed following Eq. (3). In Eq. (6), $\tilde{H}^{\pm}_{e\text{-}ph}$ is the phonon emission $(+)$ and absorption $(-)$ part of the screened EPI: $\tilde{H}_{e\text{-}ph}=\tilde{H}^{+}_{e\text{-}ph}+\tilde{H}^{-}_{e\text{-}ph}$ and

$$
\langle jk',n_{sq}\pm1|\tilde{H}^{\pm}_{e\text{-}ph}|jk,n_{sq}\rangle
$$
$$
=V_{sq}n_{sq}^{\pm\,1/2}\varepsilon_j(q_\|)^{-1}\Delta_j(q_z)\delta_{k,k'\pm q_\|}. \quad (7)
$$

Here $n_{sq}^{\pm}=n_{sq}+1/2\pm1/2$, $\mathbf{q}=(q_\|,q_z)$, $\varepsilon_j(q_\|)$ is the dielectric screening constant,

$$
\Delta_j(q_z)=\int\phi_j(z)^2\varphi_{sq}(z)dz \quad (8)
$$

is the momentum conservation factor, $\phi_j(z)$ is the confinement wave function, and $V_{sq}$ is the strength of the EPI. We consider only the bulk phonon mode $\varphi_{sq}(z)=e^{iq_z z}$. For the optical phonons, we consider only the LO phonon interaction and suppress the index $s$ from $\Delta_{sj}(q_z)=\Delta_j(q_z)$ for simplicity.

The phonon-assisted transition rate is then given by

$$
W^{ph}_{1\to2}=\frac{4\pi}{\hbar}\sum_{kk'}\sum_{sq\pm}f_{1k}(1-f_{2k'})
$$
$$
\times|T^{ph\pm}_{1k\to2k'}(sq)|^2\delta(\varepsilon_{2k'}\pm\hbar\omega_{sq}-\varepsilon_{1k}). \quad (9)
$$

The expression in Eq. (6) is simplified using the energy conservation in Eq. (9) to

$$
|T^{ph\pm}_{1k\to2k'}(sq)|^2=J^2V^2_{sq}n_{sq}^{\pm}\left|\frac{\Delta_1(q_z)\epsilon_1(q_\|)^{-1}}{\Delta-i\Gamma_{1k'}}\right.
$$
$$
\left.-\frac{\Delta_2(q_z)\epsilon_2(q_\|)^{-1}}{\Delta+i\Gamma_{2k}}\right|^2\delta_{k,k'\pm q_\|}. \quad (10)
$$

The back current can be found in a similar way:

$$
W^{ph}_{2\to1}=\frac{4\pi}{\hbar}\sum_{kk'}\sum_{sq\pm}f_{2k'}(1-f_{1k})
$$
$$
\times|T^{ph\mp}_{2k'\to1k}(sq)|^2\delta(\varepsilon_{2k'}\pm\hbar\omega_{sq}-\varepsilon_{1k}), \quad (11)
$$

with

$$
|T^{ph\mp}_{2k'\to1k}(sq)|^2=J^2V^2_{sq}n_{sq}^{\mp}\left|\frac{\Delta_1(q_z)\varepsilon_1(q_\|)^{-1}}{\Delta-i\Gamma_{1k'}}\right.
$$
$$
\left.-\frac{\Delta_2(q_z)\varepsilon_2(q_\|)^{-1}}{\Delta+i\Gamma_{2k}}\right|^2\delta_{k,k'\pm q_\|}. \quad (12)
$$

Note that the order for $+$ and $-$ is reversed in the $T$ matrix in Eqs. (11) and (12).

The phonon-assisted current is obtained by subtracting Eq. (11) from Eq. (9) and exploiting the nonequilibrium version of detailed balance: $f_{1k}(1-f_{2k'})n_{sq}^{\pm}-f_{2k'}(1-f_{1k})n_{sq}^{\mp}$ $=f_{1k}(1-f_{2k'})n_{sq}^{\pm}(1-e^{-\beta eV})$:

$$
I^{ph}=\frac{4\pi e}{\hbar}J^2F(V)\sum_{kk'}\sum_{sq\pm}f_{1k}(1-f_{2k'})
$$
$$
\times n_{sq}^{\pm}V^2_{sq}\left|\frac{\Delta_1(q_z)\epsilon_1(q_\|)^{-1}}{\Delta-i\Gamma_{1k'}}-\frac{\Delta_2(q_z)\epsilon_2(q_\|)^{-1}}{\Delta+i\Gamma_{2k}}\right|^2
$$
$$
\times\delta(\varepsilon_{2k'}\pm\hbar\omega_{sq}-\varepsilon_{1k})\delta_{k,k'\pm q_\|}. \quad (13)
$$

The cross terms in Eq. (13) yield the interference effect. This term is negligible for the phonon modes localized in one of the QW's. Short-wavelength phonons $(q_z d\gg1)$ do not contribute to this term even for the extended bulk phonons. This point is easily seen for identical confinement wave functions, for example, from $\Delta_1(q_z)^*\Delta_2(q_z)=|\Delta_1(q_z)|^2e^{iq_z d}$ ($d$ is the well-to-well separation). The summation on $q_z$ cancels out for $q_z d\gg1$. Also, the factors $\Delta_j(q_z)$ are small for $q_z b\gg1$ where $b(>d)$ is the QW width. The cross term can introduce a destructive interference for long-wavelength phonons $(q_z d\ll1)$ away from the resonance, namely, for $|\Delta|\gg\Gamma_{jk}$ for identical QW's [i.e., $\epsilon_1(q_\|)=\epsilon_2(q_\|)$]. In this case, the two terms in Eq. (13) cancel out, yielding a negligible off-resonance tunneling current. This effect arises from the fact that long-wavelength phonons modulate the energies of the two QW's in phase and do not contribute to inelastic tunneling.

## C. Tunneling through electron-electron scattering

The electrons can relax their energy and momentum by colliding with other electrons before or after tunneling as illustrated by two-step processes in Fig. 2. The initial state $|1k,jk_1\rangle=|1k\rangle|jk_1\rangle$ represents a two-particle state with an electron in $|1k\rangle$ and the other in $|jk_1\rangle$ in the $j$th OW. The final state is $|2k',jk_1'\rangle$. In Fig. 2(a), the electron in $|1k\rangle$ is first scattered into an intermediate state $|1k'\rangle$ while kicking
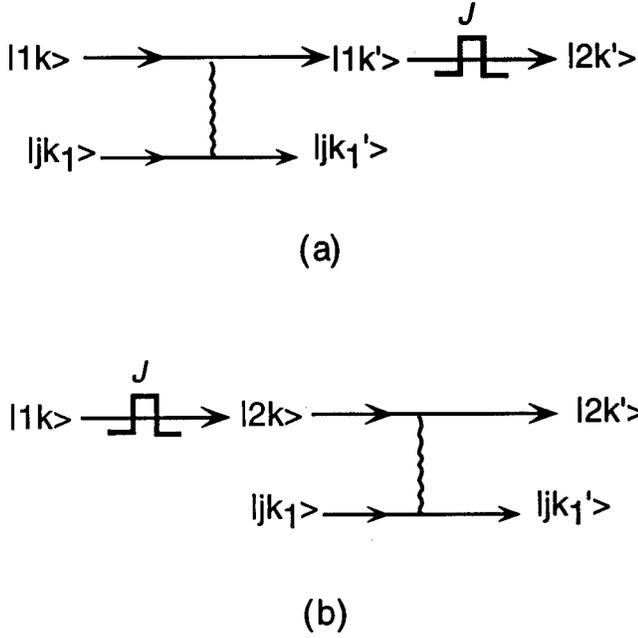
**(a)**



**(b)**

FIG. 2. Second-order two-step processes for tunneling through electron-electron interaction (wiggly vertical lines). Tunneling takes place (a) after and (b) before the interaction.

the other electron into $|jk_1'\rangle$. It then tunnels into $|2k'\rangle$. The exchange effect will be discussed later. The two steps are reversed in Fig. 1(b). In this inelastic transition, energy and momentum are transferred through an Auger-like process. The $T$ matrix for these processes is given by

$$T^{ee}_{1k,jk_1 \to 2k',jk_1'} = \frac{J\langle 1k',jk_1'|\tilde{H}_{ee}|1k,jk_1\rangle}{\varepsilon_j - \varepsilon_{1\kappa'} - i\Gamma_{1k'}(\varepsilon_j)}$$

$$+ \frac{\langle 2k',jk_1'|\tilde{H}_{ee}|2k,jk_1\rangle J}{\varepsilon_{1\kappa} - \varepsilon_{2k} - i\Gamma_{2k}(\varepsilon_{1\kappa})}, \quad (14)$$

where the quantity $\varepsilon_j$ in the first denominator is given by $\varepsilon_j = \varepsilon_{1k} + \varepsilon_{jk_1} - \varepsilon_{jk_1'} = \varepsilon_{2k'}$ with the last equality arising from the energy conservation between the final and initial state [see Eq. (15)]. The first and second denominator in Eq. (14) then simplifies to $\Delta - i\Gamma_{1k'}$ and $-\Delta - i\Gamma_{2k}$, respectively, as in the phonon-assisted case.

The tunneling rate from QW1 to QW2 equals

$$W^{ee}_{1\to 2} = \frac{8\pi}{\hbar} \sum_{jkk'} \sum_{k_1k_1'} |T^{ee}_{1k,jk_1 \to 2k',jk_1'}|^2 f_{1k}f_{jk_1}$$

$$\times (1-f_{2k'})(1-f_{jk_1'})\delta(\varepsilon_{1k} + \varepsilon_{jk_1} - \varepsilon_{2k'} - \varepsilon_{jk_1'}),$$

$$(15)$$

where the factor 8 includes spin sums. The matrix elements in Eq. (14) are given by

$$\langle ik',jk_1'|\tilde{H}_{ee}|ik,jk_1\rangle = \frac{2\pi e^2}{A\kappa q\varepsilon_{ij}(q)}F_{ij}(q)\delta_{k+k_1,k'+k_1'}$$

$$\equiv U_{ij}(q)\delta_{k+k_1,k'+k_1'}, \quad (16a)$$

where

$$F_{ij}(q) = \int\int \phi_i(z)^2\phi_j(z')^2 e^{-q|z-z'|}dz\,dz', \quad (16b)$$

$q = |k'-k|$, $\epsilon_{ij}$ is the dielectric screening constant, $\kappa$ is the bulk dielectric constant, and $A$ is the area of the QW's.

The back current can be found similarly by reversing the direction of the arrows in Fig. 2, yielding

$$W^{ee}_{2\to 1} = \frac{8\pi}{\hbar} \sum_{jkk'} \sum_{k_1k_1'} |T^{ee}_{2k',jk_1' \to 1k,jk_1}|^2 f_{2k'}f_{jk_1'}$$

$$\times (1-f_{1k})(1-f_{jk_1})\delta(\varepsilon_{1k} + \varepsilon_{jk_1} - \varepsilon_{2k'} - \varepsilon_{jk_1'}),$$

$$(17)$$

where

$$T^{ee}_{2k',jk_1' \to 1k,jk_1} = J\left(\frac{\langle 1k,jk_1|\tilde{H}_{ee}|1k',jk_1'\rangle}{\Delta - i\Gamma_{1k'}} + \frac{\langle 2k,jk_1|\tilde{H}_{ee}|2k',jk_1'\rangle}{-\Delta - i\Gamma_{2k}}\right). \quad (18)$$

The $T$ matrices in Eqs. (14) and (18) are identical in view of Eq. (16) and the discussion following Eq. (14). The energy conservation condition in Eq. (17) yields $f_{2k'}f_{jk_1'}(1-f_{1k})(1-f_{jk_1}) = f_{1k}f_{jk_1}(1-f_{2k'})(1-f_{jk_1'})e^{-\beta eV}$.

The tunneling current is then the difference between the forward current and the back current:

$$I^{ee} = \frac{8\pi}{\hbar}F(V)\sum_{jkk'} \sum_{k_1k_1'} |T^{ee}_{1k,jk_1 \to 2k',jk_1'}|^2 f_{1k}f_{jk_1}$$

$$\times (1-f_{2k'})(1-f_{jk_1'})\delta(\varepsilon_{1k} + \varepsilon_{jk_1} - \varepsilon_{2k'} - \varepsilon_{jk_1'}).$$

$$(19)$$

In the above treatment, we have assumed that the two-particle wave function is a product of the single-particle wave functions: $|ik,jk_1\rangle = |ik\rangle|jk_1\rangle$. To account for the exchange effect, we symmetrize and antisymmetrize $|ik,jk_1\rangle$ for the spin-singlet and spin-triplet states, respectively. This procedure is straightforward. We write down the result only for the most practical case where the Coulomb interaction as well as the wave function overlap between the two QW's is negligible. The net result is to replace the $T$ matrix in Eq. (19) by

$$|T^{ee}_{1k,jk_1 \to 2k',jk_1'}|^2$$

$$= J^2\left(\frac{U_{11}(k'-k)^2 - \frac{1}{2}U_{11}(k'-k)U_{11}(k_1'-k)}{\Delta^2 + \Gamma_{1k'}^2}\delta_{j,1}\right.$$

$$\left. + \frac{U_{22}(k'-k)^2 - \frac{1}{2}U_{22}(k'-k)U_{22}(k_1'-k)}{\Delta^2 + \Gamma_{2k}^2}\delta_{j,2}\right)$$

$$\times \delta_{k+k_1,k'+k_1'}. \quad (20)$$

The second terms in the numerators of Eq. (20) represent the exchange correction.

### D. Damping of the electronic states

The tunneling current studied above is a skewed Lorentzian in $V$ with the width determined by the damping of the intermediate states. Note that the current is not merely a sum of the Lorentzian functions because the phase space for tunneling increases with the bias potential $V$ until the Fermi level of QW2 aligns with the ground sublevel of QW1. Contributions to the damping of the intermediate states are given by Refs. 14–16.

$$\Gamma_{jk}^{im}(z) = \pi \sum_{k'} \langle |\langle jk'|\tilde{H}_{im}|jk\rangle|^2 \rangle_{im} \delta(\varepsilon_{jk'} - z), \quad (21a)$$

$$\Gamma_{jk}^{ph}(z) = \pi \sum_{k'} \sum_{sq\pm} [\pm f_{jk'} + n_{sq}^{\mp}][V_{sq}\Delta_j(q_z)/\varepsilon_j(q_\parallel)]^2$$

$$\times \delta(z \pm \hbar\omega_{sq} - \varepsilon_{jk'})\delta_{k,k'\pm q_\parallel}, \quad (21b)$$

and

$$\Gamma_{jk}^{ee}(z) = 2\pi \sum_{k'} \sum_{k_1 k_1'} U_{jj}(k-k')^2 f_{jk_1}(1-f_{jk'})(1-f_{jk_1'})$$

$$\times [1 + e^{-\beta(z-\mu_j)}]\delta(z + \varepsilon_{jk_1} - \varepsilon_{jk'} - \varepsilon_{jk_1'}). \quad (21c)$$

A systematic formal justification of the expressions for the tunneling current in this section as well as a formalism for higher-order corrections is given in the next section.

## III. FIELD-THEORETIC FORMALISM

In this section, we give a general formalism for the tunneling current which includes the interactions to all orders and allows a systematic evaluation of higher-order effects for the current. We then evaluate the basic lowest-order effect and rederive the results of Sec. II.

### A. Current-current correlation function

It is convenient to replace $\epsilon_{jk}$ in Eq. (1) by $\epsilon_{jk} - \mu_j$ for the following analysis. The tunneling current is given by the golden rule to the second order in $J$ in terms of the tunneling rates $W_{1\to2}$ and $W_{2\to1}$ and equals

$$I = e(W_{1\to2} - W_{2\to1}) = \frac{4\pi e}{\hbar Z} \sum_{nm} [e^{-\beta E_n}|\langle m|t^\dagger|n\rangle|^2$$

$$- e^{-\beta E_m}|\langle n|t|m\rangle|^2]\delta(E_n - E_m + \Omega), \quad (22)$$

where $E_n, |n\rangle$, and $Z$ are the eigenvalues, eigenstates, and the distribution function of $H$ and $\Omega = \mu_1 - \mu_2 = eV$. The spin degeneracy factor 2 is included in Eq. (22). The expression in Eq. (22) can be recast into a standard current-current correlation function $F(\omega_r)$

$$I = \frac{4e}{\hbar}\text{Im }F(\omega_r \to \Omega + i0): F(\omega_r) = \int_0^\beta e^{\omega_r u}\langle e^{uH}te^{-uH}t^\dagger\rangle du, \quad (23)$$
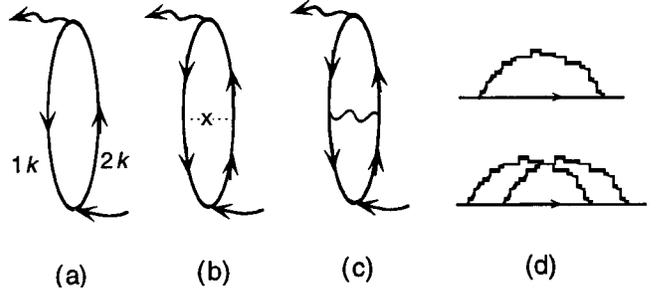


FIG. 3. Major contributions to the current correlation function. (a) Bubble diagram, (b) one-impurity-rung diagram (dashed horizontal line with a cross), (c) one-phonon-rung (wavy horizontal line) diagram, and (d) electron-electron self-energy part. The wiggly curves represent screened electron-electron interaction in the random phase approximation.

where Im means the imaginary part of the quantity that follows and the angular brackets denote the thermodynamic average. The energy parameter $\omega_r = 2\pi ri\beta^{-1}$ is on the imaginary axis and is to be analytically continued to slightly above the real axis: $\Omega + i0$ and $r$ is an integer.

### B. Tunneling current

In this section, we evaluate the leading terms in Eq. (23) using a standard diagrammatic perturbation theory.[14,15] The most important contribution comes from the basic bubble diagram shown in Fig. 3(a):

$$F(\omega_r) = -J^2\beta^{-1}\sum_{kl} G_{1k}(\zeta_l + \mu_1)G_{2k}(\zeta_l + \mu_2 + \omega_r), \quad (24)$$

where $\zeta_l = (2l+1)\pi i\beta^{-1}$, $l$ is an integer,

$$G_{jk}(\zeta_l) = \frac{1}{\zeta_l - \varepsilon_{jk} - S_{jk}(\zeta_l)} \quad (25)$$

is the dressed fermion propagator shown by the solid lines, and $S_{jk}(\zeta_l)$ is the self-energy part. Carrying out the $l$ summation in Eq. (24) and inserting the result in Eq. (23), we find

$$I' = \frac{4\pi e}{\hbar}J^2\int_{-\infty}^\infty [f_1(z) - f_2(z)]\sum_k \rho_{1k}(z)\rho_{2k}(z)dz, \quad (26)$$

where

$$\rho_{jk}(z) = \frac{1}{\pi}\frac{\Gamma_{jk}(z)}{[z - \varepsilon_{jk} - M_{jk}(z)]^2 + \Gamma_{jk}(z)^2}, \quad (27)$$

and $M_{jk}(z), \Gamma_{jk}(z)$ are the real and imaginary part of $S_{jk}(z)$. The damping part $\Gamma_{jk}(z)$ is the sum of the three contributions in Eq. (21). The real part $M_{jk}(z)$ renormalizes the single-particle energy and will not be considered in this paper. The Fermi functions in Eq. (26) are given by $f_j(z) = \{\exp[\beta(z-\mu_j)]+1\}^{-1}$. Expressions similar to that in Eq. (26) have been obtained earlier by employing Keldysh's nonequilibrium Green's function method[17] in metal-insulator-metal single-barrier tunneling structures.[18]

The compact result in Eq. (26) is more formal than the perturbation results obtained in Sec. II, although the latter contain one-rung corrections that are absent from Eq. (26) as will be shown below. Unfortunately, the expression in Eq. (26) cannot be evaluated within a reasonable computing time for realistic $\Gamma_{jk}(z)$ unless a quasiparticle approximation is made to the initial and final states, which yielded the main part of the results in Sec. II. In the following, we study the contributions to the current in Eq. (26) from the impurity, electron-phonon, and electron-electron scattering, examine the validity of the results in Sec. II and proceed to investigate the higher-order effect.

The contribution to tunneling from impurity scattering is obtained by expanding $\rho_{1k}(z)\rho_{2k}(z) \simeq [\Gamma_{1k}^{im}(z)|G_{1k}(z-i0)|^2\rho_{2k}(z) + \Gamma_{2k}^{im}(z)|G_{2k}(z-i0)|^2\rho_{1k}(z)]\pi^{-1}$ to the first order in $\Gamma_{jk}^{im}$ in Eq. (26). Using the expressions for $\Gamma_{1k}^{im}(z),\Gamma_{2k}^{im}(z)$ in Eq. (21a) and the identity $f_1(z)-f_2(z) = f_1(z)[1-f_2(z)]F(V)$ and approximating $\rho_{jk}(z) = \delta(\epsilon_{jk}-z)$, the impurity part of Eq. (26) yields

$$
I'_{im} = \frac{4\pi e}{\hbar} J^2 F(V) \sum_{kk'} f_{1k}(1-f_{2k'})
$$
$$
\times [|\langle 1k'|\tilde{H}_{im}|1k\rangle G_{1k'}(\varepsilon_{2k'}-i0)|^2
$$
$$
+ |\langle 2k'|\tilde{H}_{im}|2k\rangle G_{2k}(\varepsilon_{1k}-i0)|^2], \qquad (28)
$$

which is identical to the two terms $\propto |\langle jk'|\tilde{H}_{im}|jk\rangle|^2$ in Eq. (5).

The one-impurity-rung diagram shown in Fig. 3(b) yields

$$
I''_{im} = \frac{8\pi e}{\hbar} J^2 \int_{-\infty}^{\infty} [f_1(z)-f_2(z)] \sum_{kk'} I_{k,k'} R_{1k'}(z)\rho_{1k}(z)
$$
$$
\times [\rho_{2k}(z)R_{2k'}(z) + \rho_{2k'}(z)R_{2k}(z)]dz, \qquad (29)
$$

where $R_{jk}(z)$ is the real part of $G_{jk}(z)$ and $I_{k,k'} \equiv \langle\langle 1k'|\tilde{H}_{im}|1k\rangle\langle 2k|\tilde{H}_{im}|2k'\rangle\rangle_{im}$. To proceed further, we approximate

$$
\text{Re}\{G_{1k}(z\pm i0)G_{2k}(z\pm i0)\} \ll \text{Re}\{G_{1k}(z\mp i0)G_{2k}(z\pm i0)\}. \qquad (30)
$$

This relationship means that, when the quantities in Eq. (30) are multiplied by a slowly varying function of $\varepsilon_k$ and summed on $\varepsilon_k$, the left-hand side (LHS) gives a negligible contribution compared to the right-hand side (RHS). The basic reason is that any contribution, to be significant, should arise from the region near the poles $\varepsilon_{1k}=z\pm i\Gamma_{1k}$, $\varepsilon_{2k}=z \pm i\Gamma_{2k}$ (assuming a constant $\Gamma_{jk}$). For the quantity on the LHS, the integration contour can be closed on the complex plane to enclose zero poles, yielding a vanishing contribution since the poles are on the same side. This is not possible for the RHS, which has a sharp Lorentzian resonance when the two QW sublevels align. An alternate perturbative argument was given earlier.[14] With this approximation, Eq. (29) yields

$$
I''_{im} = \frac{8\pi e}{\hbar} J^2 \int_{-\infty}^{\infty} [f_1(z)-f_2(z)] \sum_{kk'} \langle\langle 1k'|\tilde{H}_{im}|1k\rangle
$$
$$
\times \langle 2k|\tilde{H}_{im}|2k'\rangle\rangle_{im}
$$
$$
\times \rho_{1k}(z)\rho_{2k'}(z)\text{Re}\{G_{1k'}(z-i0)G_{2k}(z+i0)\}dz. \qquad (31)
$$

This result reduces to the cross terms in Eq. (5) in the limit $\rho_{1k}(z) = \delta(\varepsilon_{1k}-z)$ and $\rho_{2k'}(z) = \delta(\varepsilon_{2k'}-z)$. These terms contribute only when the impurities reside in the center barrier.

The contribution from the phonon-assisted tunneling to Eq. (26) is obtained by expanding $\rho_{1k}(z)\rho_{2k}(z) = [\Gamma_{1k}^{ph}(z)|G_{1k}(z-i0)|^2\rho_{2k}(z) + \Gamma_{2k}^{ph}(z)|G_{2k}(z-i0)|^2\rho_{1k}(z)]\pi^{-1}$ to the first order in $\Gamma_{jk}^{ph}$ in Eq. (26). Using the expressions for $\Gamma_{1k}^{ph}(z),\Gamma_{2k}^{ph}(z)$ in Eq. (21b) and the identity $\pm f_{jk'} + n_{sq}^{\mp} = f_{jk'}n_{sq}^{\pm}f_j(z)^{-1}$ and approximating $\rho_{jk}(z) = \delta(\varepsilon_{jk}-z)$, we find

$$
I'_{ph} = \frac{4\pi e}{\hbar} J^2 F(V) \sum_{kk'} f_{1k}(1-f_{2k'})
$$
$$
\times \sum_{sq\pm} n_{sq}^{\mp} V_{sq}^2 \{|\Delta_1(q_z)G_{1k'}(\varepsilon_{2k'}-i0)/\epsilon_1(q_\parallel)|^2
$$
$$
+ |\Delta_2(q_z)G_{2k}(\varepsilon_{1k}-i0)/\epsilon_2(q_\parallel)|^2\}
$$
$$
\times \delta(\varepsilon_{2k'}-\varepsilon_{1k}\pm\hbar\omega_{sq})\delta_{k,k'\pm q_\parallel}. \qquad (32)
$$

This contribution is to be identified with the two direct terms in Eq. (13).

The cross terms in Eq. (13) arise from the one-phonon-rung diagram shown in Fig. 3(c) which reads

$$
F''_{ph}(\omega_r) = -j^2\beta^{-2} \sum_{kk'll'} \sum_{sq\pm} \frac{V_{sq}^2\Delta_1(q_z)\Delta_2(q_z)}{\epsilon_1(q_\parallel)\epsilon_2(q_\parallel)[\hbar\omega_{sq}\pm(\zeta_l-\zeta_{l'})]}
$$
$$
\times G_{1k}(\zeta_l+\mu_1)G_{2k}(\zeta_l+\mu_2+\omega_r)
$$
$$
\times G_{1k'}(\zeta_{l'}+\mu_1)G_{2k'}(\zeta_{l'}+\mu_2+\omega_r)\delta_{k',k+q_\parallel}. \qquad (33)
$$

The quantity $\delta_{k',k+q_\parallel}$ here can be replaced by $\delta_{k',k-q_\parallel}$ due to the in-plane inversion symmetry. An inversion symmetry in the growth direction $\phi_j(z)^2 = \phi_j(-z)^2$ simplifies $\Delta_j(q_z)$ to

$$
\Delta_j(q_z) = \int_{-\infty}^{\infty} \phi_j^2(z)\cos(q_z z)dz. \qquad (34)
$$

The $l$ and $l'$ summations in Eq. (33) are converted into contour integrations on the complex plane. These integrations generate many terms which contain the factors shown in Eq. (30). After a lengthy calculation and employing the approximation given in Eq. (30), we obtain,

$$I''_{\mathrm{ph}} = \frac{8\pi e}{\hbar} J^2 F(V) \int_{-\infty}^{\infty} dz \int_{-\infty}^{\infty} dx\, f_1(z)[1-f_2(x)]$$

$$\times \sum_{kk'} \rho_{1k}(z)\rho_{2k'}(x) \sum_{sq\pm} n_{sq}^{\pm} V_{sq}^2$$

$$\times \frac{\Delta_1(q_z)\Delta_2(q_z)}{\epsilon_1(q_{\parallel})\epsilon_2(q_{\parallel})} \mathrm{Re}\{G_{1k'}(x-i0)G_{2k}(z+i0)\}$$

$$\times \delta(x-z\pm\hbar\omega_{sq})\delta_{k,k'\pm q_{\parallel}}. \tag{35}$$

Combining Eqs. (32) and (35), we find

$$I'_{\mathrm{ph}} = \frac{4\pi e}{\hbar} J^2 F(V) \int_{-\infty}^{\infty} dz \int_{-\infty}^{\infty} dx\, f_1(z)[1-f_2(x)]$$

$$\times \sum_{kk'} \rho_{1k}(z)\rho_{2k'}(x) \sum_{sq\pm} n_{sq}^{\pm} V_{sq}^2 |\Delta_1(q_z)$$

$$\times G_{1k'}(x-i0)/\varepsilon_l(q_{\parallel}) + \Delta_2(q_z)G_{2k}(z+i0)/\varepsilon_2(q_{\parallel})|^2$$

$$\times \delta(x-z\pm\hbar\omega_{sq})\delta_{k,k'\pm q_{\parallel}}. \tag{36}$$

This result is identical to the phonon-assisted tunneling current obtained in Eq. (13) in the limit $\rho_{1k}(z)=\delta(z-\varepsilon_{1k})$ and $\rho_{2k'}(z)=\delta(z-\varepsilon_{2k'})$.

The contribution from electron-electron scattering to Eq. (26) is obtained by expanding

$$\rho_{1k}(z)\rho_{2k}(z) = [\Gamma_{1k}^{ee}(z)|G_{1k}(z-i0)|^2 \rho_{2k}(z)$$

$$+ \Gamma_{2k}^{ee}(z)|G_{2k}(z-i0)|^2 \rho_{1k}(z)]\pi^{-1}$$

to the first order in $\Gamma_{jk}^{ee}$ in Eq. (26). Using the expressions for $\Gamma_{1k}^{ee}(z), \Gamma_{2k}^{ee}(z)$ in Eq. (21c) and approximating $\rho_{jk}(z) = \delta(\varepsilon_{jk}-z)$, we find

$$I'_{ee} = \frac{8\pi e}{\hbar} J^2 F(V) \sum_{jkk_1} \sum_{k'k'_1} f_{1k}f_{jk_1}(1-f_{2k'})(1-f_{jk'_1})$$

$$\times \delta(\varepsilon'_{1k}+\varepsilon_{jk_1}-\varepsilon_{2k'}-\varepsilon_{jk'_1})$$

$$\times [|U_{11}(k'-k)G_{1k'}(\varepsilon_{2k'}-i0)|^2 \delta_{j,1}$$

$$+ |U_{22}(k'-k)G_{2k}(\varepsilon_{1k}-i0)|^2 \delta_{j,2}]. \tag{37}$$

This contribution is to be identified with the direct terms in Eqs. (19) and (20). The rung correction to Eq. (37) arises from inter-QW Coulomb interaction and is small. The electron-electron self-energy part in Eq. (21c) is given by the upper part of Fig. 3(d) where the wiggly curve denotes a dressed electron-electron interaction. The lower part of Fig. 3(d) can be included in Eq. (37) by replacing $U_{jj}(k'-k)^2 \rightarrow U_{jj}(k'-k)^2 - U_{jj}(k'-k)U_{jj}(k'_1-k)/2$.

The phonon rung in the present tunneling problem gives a relatively smaller correction compared with the single-QW or bulk transport problem, because each of the two EPI vertices originate from different QW's, yielding $\Delta_1(q_z)^*\Delta_2(q_z)=|\Delta_1(q)_z|^2 e^{iq_z d}$. A significant amount of contribution from the $q_z$ integration arises only from a restricted region $q_z \leqslant 1/d$ as discussed already in Sec. II. In view of the fact that $d$ is large in tunneling structures, successive rung diagrams are expected to converge rapidly.

Also, the impurity-rung correction can be important only when the impurities are in the center barrier close to the wave functions in both wells.

## IV. NUMERICAL EVALUATION

In this section, we evaluate the tunneling current in GaAs/Al$_{0.3}$Ga$_{0.7}$AsDQW's with 120-Å-wide QW's separated by a 125-Å-wide center barrier and compare with recent data.[11] The electron densities of the QW's are $N_1=8$ and $N_2=2\times10^{11}\,\mathrm{cm}^{-2}$, yielding the Fermi energies $\varepsilon_{1F}=28.7\,\mathrm{meV}$, $\varepsilon_{2F}=7.2\,\mathrm{meV}$, and $\Delta=21.5\,\mathrm{meV}$ at zero bias for an effective mass $m^*=0.067$ (in units of free electron mass) in the wells. The dimension of the geometric tunneling area of the sample is $L_x=0.02\,\mathrm{cm}$, $L_y=0.05\,\mathrm{cm}$. The center barrier is dopant free, yielding a negligible contribution from the cross term in Eq. (5) and

$$I^{\mathrm{im}} = \frac{4eJ^2}{\hbar} F(V) \sum_k \left[ f_1(\varepsilon_{2k})(1-f_{2k}) \frac{\Gamma_{1k}^{\mathrm{im}}(\varepsilon_{2k})}{\Delta^2+\Gamma_{1k}^2} \right.$$

$$\left. + f_{1k}(1-f_2(\varepsilon_{1k})) \frac{\Gamma_{2k}^{\mathrm{im}}(\varepsilon_{1k})}{\Delta^2+\Gamma_{2k}^2} \right]. \tag{38}$$

Here, damping $\Gamma_{jk}^{\mathrm{im}}(z)$ in the numerators was defined in Eq. (21a) and is an impurity part of $\Gamma_{jk}$ in the denominators. The quantity $\Gamma_{jk}^{\mathrm{im}}(z)$ follows from summing on one of the dummy wave numbers in Eq. (5). The Fermi function $f_j(z)$ was defined following Eq. (27).

For a numerical evaluation, we ignore the momentum dependence of the impurity scattering (relevant for short-range scattering) and approximate $\Gamma_{jk}^{\mathrm{im}}(z)$ as a constant $\Gamma_{jk}^{\mathrm{im}}(z) \simeq \Gamma_j^{\mathrm{im}}$ above the band bottom and zero otherwise. This approximation as well as neglecting the cross term in Eq. (38) is also valid for interface-roughness scattering. Therefore, $\Gamma_j^{\mathrm{im}}$ contains the contribution from interface-roughness scattering. The quantities $\Gamma_j^{\mathrm{im}}$ depend on the doping configuration and the sample quality. Since the doping configuration and the degree of interface roughness is not well known for our sample, these quantities are taken as adjustable parameters for comparison with the data. However, $\Gamma_1^{\mathrm{im}}$ and $\Gamma_2^{\mathrm{im}}$ will be scaled inversely with the mobilities of QW1 and QW2, respectively, thereby leaving only one adjustable parameter. Other damping parameters in $\Gamma_{jk}$ from electron-electron and electron-phonon scattering are calculated microscopically without any adjustable parameters.

The EPI with the LO phonons are given by

$$V_{q,\mathrm{LO}} = \left( \frac{4\pi\eta\hbar^{5/2}\omega_q^{3/2}}{\Omega_{vol}q^2\sqrt{2m^*}} \right)^{1/2}, \tag{39}$$

where $\Omega_{\mathrm{vol}}$ is the sample volume and $\eta=0.06$ is the dimensionless coupling parameter for GaAs QW's. The dispersion of the optical phonon frequency will be ignored: $\hbar\omega_q \equiv \hbar\omega_o=36.2\,\mathrm{meV}$. The electrons interact with the acoustic phonons through screened deformation potential scattering and piezoelectric scattering with the parameters given in Ref. 19. The dielectric screening constant is approximated by

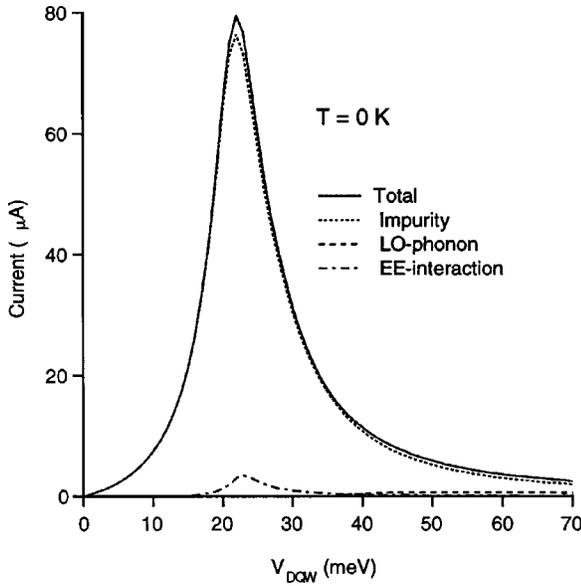$$\epsilon_j(q_{\parallel}) = (1+sq_{\parallel}^{-1}F_{ij}(q_{\parallel})[1-e^{-T_{jF}/T}])^{-1}, \tag{40}$$

FIG. 4. Tunneling current as a function of the voltage drop between the layers at 0 K.

where $T_{jF}$ is the Fermi temperature, $s = 2e^2 m^*/\kappa\hbar^2$ is the screening constant, and $\kappa = 13$.

The $I$-$V$ curves are calculated using the results in Sec. II and employing an adjustable parameter $J = 0.001$ meV, $\Gamma_1^{im} = 4$ meV, and $\Gamma_2^{im} = 12$ meV. The ratio of $\Gamma_1^{im}$ and $\Gamma_2^{im}$ here equals the measured ratio of the low-temperature mobilities $\mu_2/\mu_1$ of the sample. The calculated $I$-$V$ curves are displayed in Figs. 4–7 as a function of the voltage drop $V_{DQW}$ across the barrier for $T = 0$, 77, and 300 K. The $I$-$V_{DQW}$ curve at 77 K in Fig. 5 is similar to the experimentally observed $I$-$V_{SD}$ curve in shape and magnitude[11] except that the experimental $I$-$V_{SD}$ curve is skewed slightly toward the right due to the fact that (1) $V_{SD}$ is the sum of $V_{DQW}$ and the in-plane voltage drop $V_\parallel$ in the QW's, neglected in the present treatment, and (2) $V_\parallel$ is larger for a larger current. A

tight-binding estimate of $J$ based on a simple flat-band potential yields $J = 0.002$ meV for the sample, twice the $J = 0.001$ meV employed. A self-consistent Hartree calculation which includes band bending pulls the confinement wave functions in QW1 and QW2 away from each other and is expected to reduce $J$. Also, the actual tunneling area may be smaller than the geometric area $= 0.02 \times 0.05$ cm$^2$ employed for the calculation.[6] In a more realistic calculation with a known dopant distribution for the sample, the $V_{DQW}$ dependent $J$ can be calculated using a self-consistent density functional theory.

Figure 4 shows the $I$-$V_{DQW}$ curve at 0 K. The current arises primarily from impurity scattering (dotted curve). The
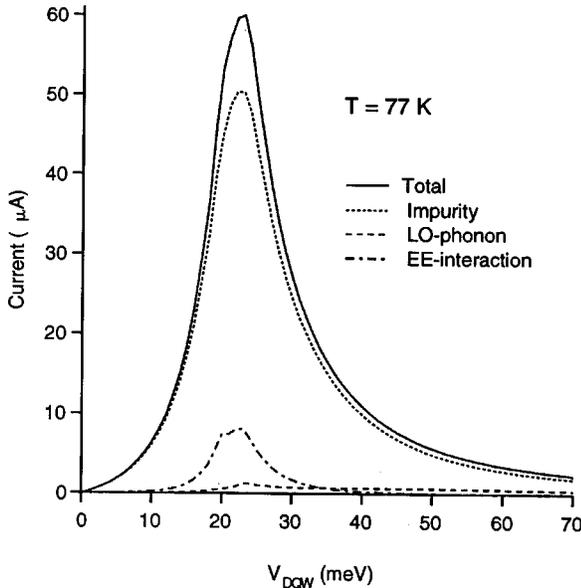


FIG. 6. Tunneling current as a function of the voltage drop between the layers at 300 K.



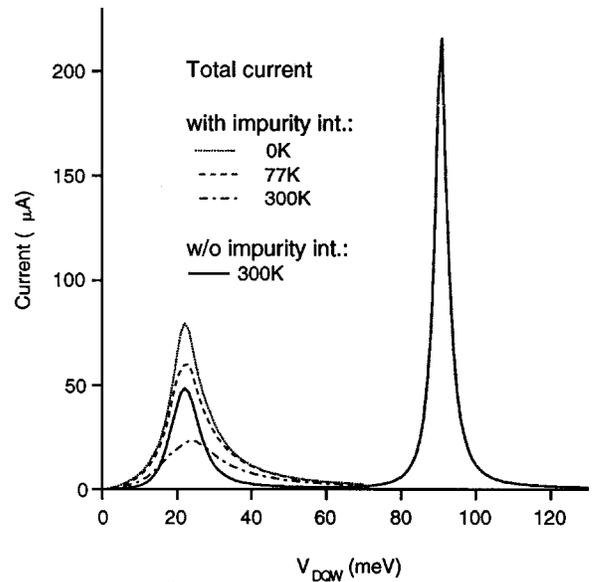FIG. 5. Tunneling current as a function of the voltage drop between the layers at 77 K.



FIG. 7. Total tunneling current as a function of the voltage between the layers at $T = 0$, 77, and 300 K. The solid curve represents the intrinsic total current at 300 K in the absence of impurity scattering and includes tunneling from the ground sublevel of QW1 to the second sublevel of QW2.

peak occurs slightly above $eV_{DQW} = \varepsilon_{1F} - \varepsilon_{2F} = 21.5$ meV where the two QW ground sublevels align. It is interesting to note that electron-electron scattering (dash-dotted curve) also contributes significantly. The small LO-phonon contribution (dashed curve) increases until the Fermi level of QW2 is about $\hbar\omega_o = 36.2$ meV below the bottom of the QW1 band (i.e., $eV = \hbar\omega_o + \varepsilon_{1F} = 64.9$ meV), where all the electrons in QW1 can tunnel into QW2 by emitting one LO phonon. The acoustic-phonon contribution, included in the total current, is the least important for the nonequilibrium tunneling current at all temperatures and is not indicated separately, although it is more important than the LO-phonon contribution at low temperatures in the linear regime. A similar result was obtained earlier for double-barrier tunneling.[9]

At 77 K, the $I$-$V_{DQW}$ curve is broader and the peak current is much smaller than at $T = 0$ K as shown in Fig. 5. The LO-phonon scattering contribution is larger than at 0 K but is still smaller than the contributions from impurity and electron-electron scattering. At 300 K, the LO-phonon and electron-electron contribution have increased considerably relative to the impurity contribution as seen in Fig. 6. It is interesting to note that the electron-electron contribution is larger than the LO-phonon contribution. This is not surprising because electron-electron scattering can cause a significant quasihole lifetime broadening (of the order of a few meV) deep under the Fermi level in QW's where the electrons are confined in a narrow space.[16] This broadening becomes small near the Fermi level in a single QW due to the limited phase space imposed by simultaneous energy and momentum conservation.[16] However, it remains large at the Fermi level in our tunneling problem, because an electron at the Fermi level can excite other electrons above the Fermi level and can still conserve the energy by tunneling into QW2 with a lower Fermi level. In contrast, electron-electron scattering does not affect the mobility directly unlike LO-phonon scattering because it conserves the momentum, as is well known. The electron density $N_1$ in the top QW (i.e., QW1) can be varied through changing the top-control-gate bias in DELTT while keeping $N_2$ nearly unchanged.[11] The peak position of the $I$-$V$ curve $eV = \Delta_o$ is proportional to $N_1 - N_2$ and increases with $N_1$. Also, the relative contribution from electron-electron scattering to the current and the width increases.

The impurity contribution is large in Fig. 6 because of the large impurity damping $\Gamma_1^{im} = 4$ meV and $\Gamma_2^{im} = 12$ meV chosen to simulate the 77 K experimental data in Ref. 11. This kind of large impurity damping is readily caused by charged impurities in modulation doped QW's which can yield large photoluminescence linewidths.[20] For rough interfaces, the contribution from roughness scattering can also contribute significantly to $\Gamma_1^{im}$ as will be shown later.

The current becomes much sharper as a function of $V$ and increases in magnitude without impurity scattering as shown by the fine-dotted curve in Fig. 6. The temperature dependence of the total tunneling current is plotted in Fig. 7. The solid curve shows the total current at 300 K in the intrinsic limit, namely, in the absence of impurity scattering (i.e., $\Gamma_1^{im} = \Gamma_2^{im} = 0$). This curve is much above the dash-dotted curve which includes the contribution from impurity scattering. The resonance at about 90 mV for the intrinsic $I$-$V$

curve represents the current from tunneling between the ground sublevel of QW1 and the second sublevel of QW2, using the same $J$ value for comparison with the first resonance current. The actual tunneling integral for this case is expected to be larger than that between the ground sublevels.

We now study the interface roughness contribution to damping. For an infinitely deep QW with a width $b_j$, the ground-sublevel-energy fluctuation in the $j$th QW is given by $\delta E_j(\mathbf{r}) = -\pi^2\hbar^2 \delta b_j(\mathbf{r})/(m^* b_j^3)$, where $\delta b_j(\mathbf{r})$ is the fluctuation of $b_j$ at position $\mathbf{r}$. Defining the correlation length $\Lambda_j$ through the average $\langle \delta b_j(\mathbf{r}) \delta b_j(\mathbf{r}') \rangle = (\delta b_j)^2 \exp(-|\mathbf{r}' - \mathbf{r}|^2/\Lambda_j^2)$ (Ref. 21) and using the golden rule, we find

$$\Gamma_{jk}^r(z) = \pi \sum_{k'} \langle |\langle j,k'|\delta E_j(\mathbf{r})|j,k\rangle|^2 \rangle \delta(\varepsilon_{jk'} - z)$$

$$= \Gamma_{rj} \int_0^{2\pi} \frac{d\phi}{2\pi} e^{-(\mathbf{k}'-\mathbf{k})^2\Lambda_j^2/4}, \tag{41}$$

where $\phi$ is the angle of $\mathbf{k}'$, $\Gamma_{rj} = \pi^5(\hbar^2/2m^* b_j^2)(\delta b_j/b_j)^2(\Lambda_j/b_j)^2$, $\varepsilon_{1k} = \hbar^2 k^2/2m^*$, and $\varepsilon_{2k} = \varepsilon_{1k} + \Delta$. The origin of the energy is at $k = 0$, namely, at the bottom of QW1, $\varepsilon_{1k} = 0$. For QW1, $\Gamma_{1k}^r(z)$ in Eq. (41) vanishes for $z < 0$ and $k'$ is fixed by $\hbar^2 k'^2/2m^* = z$. For QW2, $\Gamma_{2k}^r(z)$ in Eq. (41) vanishes for $z < \Delta$ and $k'$ is fixed by $\hbar^2 k'^2/2m^* = z - \Delta$. For a two-layer fluctuation $\delta b_j = 10$ Å out of $b_j = 120$ Å we estimate $\Gamma_{rj} = 8.40(\Lambda_j/b_j)^2$ meV. The quantities of interest are $\Gamma_{1k}^r(\varepsilon_{2k})$ and $\Gamma_{2k}^r(\varepsilon_{1k})$ in the numerators of Eq. (38). We now estimate these quantities near the resonance (i.e., $\Delta = 0$) where the most important contribution to the current arises. For $\Gamma_{1k}^r(\varepsilon_{2k})$, the Fermi functions there restrict the contribution to $0 < \mu_2 < z = \varepsilon_{2k} = \varepsilon_{1k} < \mu_1$. Therefore $|\mathbf{k}|, |\mathbf{k}'| < k_{1F} = 0.0224$ Å$^{-1}$ in Eq. (41) for our sample density $N_1 = 8 \times 10^{11}$ cm$^{-2}$. For theses values of $|\mathbf{k}|$ and $|\mathbf{k}'|$, the integral in Eq. (41) is unity, the upper limit for $\Lambda_1 \lesssim 89$ Å. The same result is obtained for $\Gamma_{2k}^r(\varepsilon_{1k})$, yielding $\Gamma_{1k}^r(\varepsilon_{2k}) = 8.40(\Lambda_1/b_1)^2$ meV and $\Gamma_{2k}^r(\varepsilon_{1k}) = 8.40(\Lambda_2/b_2)^2$ meV for $\Lambda_1, \Lambda_1 \lesssim 89$ Å. These quantities are to be added to $\Gamma_1^{im}$ and $\Gamma_2^{im}$. For $\Lambda_j = 10$ Å, we find negligible damping $\Gamma_{jk}^r = 0.058$ meV, while a large correlation length $\Lambda_j = 50$ Å yields significant damping $\Gamma_{jk}^r = 1.5$ meV. The interface-roughness contribution therefore depends on $\delta b_j$, $b_j$, and $\Lambda_j$.

## V. CONCLUSIONS

We presented a theory for nonequilibrium 2D-2D tunneling between double electron layers separated by a wide barrier when the chemical potentials of the two electron gases are arbitrarily biased. Initially, an intuitive but rigorous second-order perturbation theory was established based on a transition-rate approach. The result was used for a numerical evaluation of the $I$-$V$ relationship. Contributions from electron-impurity, electron-electron, and electron-phonon interactions have been considered. The validity of this treatment was examined using a field-theoretic formalism by expressing the tunneling current as a velocity-velocity correlation function. The correlation function was then evaluated employing a standard temperature-ordered Green's function technique. The formalism is exact to the second order in the tunneling integral and to all orders in the inter-

actions. It is similar to that of a linear response theory and useful for a systematic study of higher-order effects. The numerical results were compared with recent experimental data from GaAs/Al$_x$Ga$_{1-x}$As double quantum wells at 77 K. These data show a large peak-to-valley ratio in the $I$-$V$ curve, yielding a demonstration of a DELTT at 77 K. Numerically, a large peak-to-valley ratio was obtained at 300 K predicting the feasibility of room-temperature DELTT's.

[1] J. Smoliner, W. Demmerle, G. Berthold, E. Gornick, G. Weiman, and W. Schlapp, Phys. Rev. Lett. **63**, 2116 (1989).

[2] E. E. Mendez and L. L. Chang, Surf. Sci. **229**, 173 (1990).

[3] J. P. Eisenstein, L. N. Pfeiffer, and K. W. West, Appl. Phys. Lett. **57**, 2324 (1990).

[4] J. P. Eisenstein, T. J. Gramila, L. N. Pfeiffer, and K. W. West, Phys. Rev. B **44**, 6511 (1991).

[5] J. A. Simmons, S. K. Lyo, J. F. Klem, M. E. Sherwin, and J. R. Wendt, Phys. Rev. B **47**, 15 741 (1993).

[6] S. K. Lyo and J. A. Simmons, J. Phys.: Condens. Matter **5**, L299 (1993).

[7] L. Zheng and A. H. MacDonald, Phys. Rev. B **47**, 10 619 (1993).

[8] R. K. Hayden, D. K. Maude, L. Eaves, E. C. Valadares, M. Henini, F. W. Sheard, O. H. Hughes, J. C. Portal, and L. Curry, Phys. Rev. Lett. **66**, 1749 (1991).

[9] F. Chevoir and B. Vinter, Phys. Rev. B **47**, 7260 (1993).

[10] W. T. Dietz and R. B. Darling, Phys. Rev. B **53**, 3925 (1996).

[11] J. A. Simmons, M. A. Blount, J. S. Moon, S. K. Lyo, W. E. Baca, J. R. Wendt, J. L. Reno, and M. J. Hafich, J. Appl. Phys. **84**, 5626 (1998).

[12] P. H. Rivera and P. A. Schulz, Appl. Phys. Lett. **67**, 2675 (1995).

[13] W. Heitler, *The Quantum Theory of Radiation*, 3rd ed. (Oxford Press, Oxford, U.K., 1966), p. 163.

[14] T. Holstein, Ann. Phys. (N.Y.) **29**, 410 (1964).

[15] A. L. Fetter and J. D. Walecka, *Quantum Theory of Many-Particle Systems* (McGraw-Hill, New York, 1971).

[16] S. K. Lyo, Phys. Rev. B **43**, 7091 (1991).

[17] L. V. Keldysh, Zh. Eksp. Teor. Fiz. **47**, 1515 (1964) [Sov. Phys. JETP **20**, 1018 (1965)].

[18] C. Caroli, R. Combescot, P. Noziers, and D. Saint-James, J. Phys. C **4**, 916 (1971).

[19] S. K. Lyo, Phys. Rev. B **40**, 6458 (1989).

[20] S. K. Lyo and E. D. Jones, Phys. Rev. B **38**, 4113 (1988).

[21] H. Sasaki, T. Noda, K. Hirakawa, M. Tanaka, and T. Matsusue, Appl. Phys. Lett. **51**, 1934 (1987).